Molecular Rulers for Scaling Down Nanostructures

A. Hatzor and P. S. Weiss*

A method of constructing $<$30-nanometer structures in close proximity with precise spacings is presented that uses the step-by-step application of organic molecules and metal ions as size-controlled resists on predetermined patterns, such as those formed by electron-beam lithography. The organic molecules serve as a ruler for scaling down a larger "parent" structure. After metal deposition and lift-off of the organic multilayer resist, an isolated smaller structure remains on the surface. This approach is used to form thin parallel wires (15 to 70 nanometers in width and 1 micrometer long) of controlled thickness and spacing. The structures obtained were imaged with field emission scanning electron microscopy. A variety of nanostructures could be scaled down, including structures with hollow patterns.

Construction of well-defined sub–100-nm continuous structures on surfaces is of great importance to the fabrication of advanced electronic and opto-electronic devices. Among the most widely used techniques are electron-beam lithography (EBL) (*1*, *2*), molding (*3*), scanning probe microscopy (SPM) (*4*–*6*), nanotube assembly (*7*–*9*), rod assembly (*10*), membrane tubes deposition (*11*), and metal-coated DNA (*12*). Yet, the commonly used methods are limited in several aspects: EBL is often limited in resolution below 100 nm because of proximity effects that cause broadening and merging within the desired pattern. Higher resolution methods tend to be less flexible (*13*). The serial nature of SPM methods, even in multitip modes, limits the construction of macroscopic arrays. Nanotubes, membrane tubes, and rods are limited to predetermined widths and properties, and their ordered alignment on surfaces requires special techniques.

In many device applications, only certain structures (such as gates in transistors) have sub–100-nm dimensions within a structure with larger features. We considered whether the flexibility of methods such as EBL could be extended to higher resolution through molecular self-assembly. We demonstrated a controlled-size molecular resist that is built sideways from preformed EBL structures. The molecular resist used here decreases the gap quantitatively between two Au nanostructures. A second metal deposition is then performed on top of the molecular resist into the remaining gap. Lift-off (dissolution) of the molecular resist leaves a thin (15 to 70 nm) trace parallel to the parent gold nanofabricated structures. The study was performed on a thermally oxidized, highly polished doped Si(100) on which 1000-nm-wide parallel traces were fabricated with EBL to have 40- to 110-nm spacings. We first deposited 5-nm-thick Ti layers on Si and then 20-nm-thick Au layers.

The resist used to cover the Au traces and to pattern the gaps in between them was prepared from metal-organic coordinated multilayers (*14*). The multilayers were constructed layer-by-layer on the Au traces as described by Evans *et al.* (*15*). The organic molecule used was a mercaptoalkanoic acid. The layers were connected by Cu^{2+} ions. In a preliminary experiment, multilayer construction was carried out on both Au and oxidized Si substrates to confirm the selective construction on Au; multilayer construction on SiO$_2$ would have prevented gap formation between the Au parent traces. These control experiments were also performed to evaluate the thickness of the multilayer versus the number of layers. A bare Si substrate was also measured in x-ray photoelectron spectroscopy (XPS) as a reference for the amount of carbon present on a clean Si wafer (with native oxide on the surface) (*16*). Ellipsometry measurements yielded a thickness of 18 ± 0.5 nm for nine mercaptoalkanoic acid layers on Au (an average thickness of 2 nm per layer was measured for each processing step during multilayer construction). On a Si wafer substrate capped with an oxide, the ellipsometric parameters show no significant change after the adsorption steps. This result verifies that essentially no adsorption of these multilayers occurs on oxidized Si.

A set of 20-nm-thick multilayers (10 layers) was constructed on the Au-patterned surfaces (Fig. 1B). A second deposition was carried out with 4.5-nm Ti and 4.5-nm Au on top of the multilayer-processed substrate (Fig. 1C). The samples were then sonicated in a hot solution of 0.06 M HCl in 75% dimethylformamide (DMF) to remove both the resist and the metal that was deposited on top of the resist surface (Fig. 1D) (*17*). The resist removal was first checked by immersing the nine-layer mercaptoalkanoic acid–coated Au sample in an HCl/DMF solution and monitoring its thickness by ellipsometry. After 1 hour in solution, the thickness of the multilayer on Au was reduced from 18 to 2 nm, indicating the removal of all but the first molecular layer.

Long continuous metal wires can be formed in the gap between the pre-fabricated Au traces. Figure 2 shows the stages of the actual process in plan view for the construction of 1-μm wires that are 65- (Fig. 2, A to D) and 25-nm wide (Fig. 2, E to H). The size of the gap ($\sim$20 nm in Fig. 2D) is in good agreement with the thickness of the 10-layer molecular resist. Imaging at high resolution with scanning electron microscopy (SEM) shows no evidence of metal in these gaps. The difference between the gap size shown in Fig. 2, B and C, likely neglects the variation in field-emission SEM (FESEM) image quality for uncoated and metal-coated organic films, which enhances the resolution of the multilayer edge in Fig. 2C (*18*). Comparison of the two data sets shows the correlation between the number of layers constructed and the gap width formed (*19*).

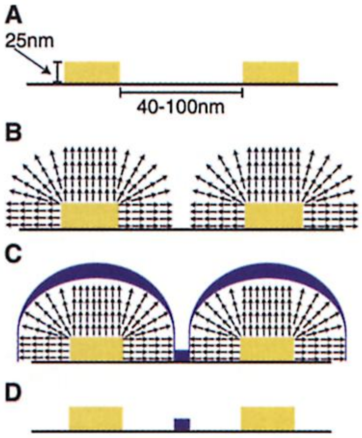

Fig. 1. Schematic of the scaling-down process. **(A)** EBL forms the parent structures (yellow rectangles). **(B)** Layer-by-layer construction of metal-organic resist (2 nm per layer). The arrows represent the mercaptoalkanoic acid (tail is the SH group); Cu^{2+} ions are not depicted. **(C)** Metal (blue arcs and rectangle) evaporation into the gap (the gap size is determined by the number of organic layers deposited). **(D)** Lift-off of the organic layer in HCl/DMF solution. The thin Ti layer was omitted for clarity.

Department of Chemistry, Penn State University, University Park, PA, 16802–6300, USA.

*To whom correspondence should be addressed. E-mail: stm@psu.edu

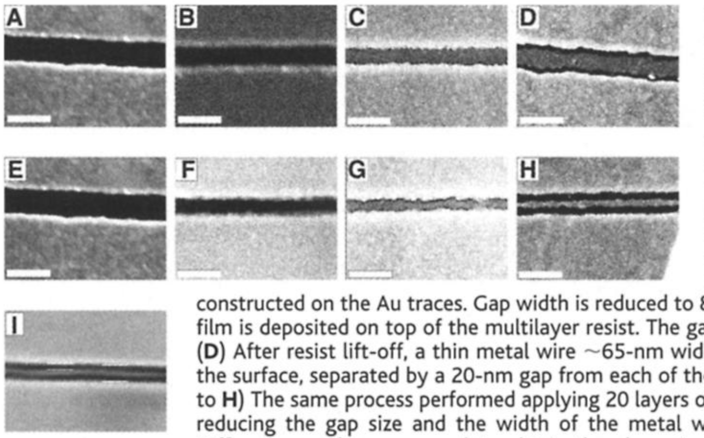

Fig. 2. FESEM images of the scaling down process. (**A**) "Parent" gold traces (bright) on oxidized Si (dark). The measured spacings between the pads is ~110 nm. (**B**) A 10-layer molecular ruler resist comprised of mercaptoalkanoic acid with a Cu^{2+} linker, constructed on the Au traces. Gap width is reduced to 80 nm. (**C**) A thin Ti/Au film is deposited on top of the multilayer resist. The gap width is now 66 nm. (**D**) After resist lift-off, a thin metal wire ~65-nm wide, 1-μm long is left on the surface, separated by a 20-nm gap from each of the parent gold traces. (**E** to **H**) The same process performed applying 20 layers of molecular resist, thus reducing the gap size and the width of the metal wire formed to 25 nm. Different samples were used to obtain the above images in order to avoid damage during imaging due to the microscope's electron beam. White bar in each image, 200 nm. (**I**) High-resolution FESEM image of a continuous, thin daughter trace placed between two parent electrodes 48-nm apart (gap shown on the right). The target gap separation was 18 nm, within experimental error of the 16-nm gap found (gap shown on the left).

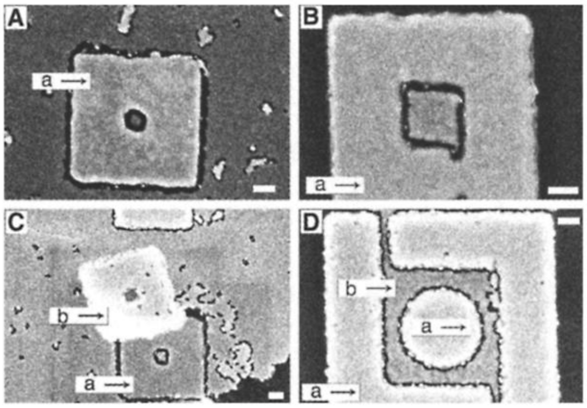

Fig. 3. A series of FESEM images showing gold dots of different size and shape and a gold ring formed in the center of hollow parent structures. Bars, 100 nm. (**A**) Parent hollow gold square on oxidized Si (arrow a). The circle in the center was formed by the second gold evaporation. The gap between the circle and the hollow square is the result of the lift-off process. (**B**) "Parent" gold hollow square of a different hole size (arrow a). The square in the center was formed similarly to the circle shown in (A). (**C**) Arrow b shows the second gold layer that was lifted as one piece from the parent gold hollow square (arrow a). The small gold square in the center of the hollow parent structure was formed by the second gold evaporation. Note the dimensions of the lifted layer that reflect the parent structure size plus the multilayer addition. (**D**) The scaling-down process forms a gold ring (arrow b) connected to two thin gold channels on opposite sides. The gold channel size is ~15 nm. The ring and channels are formed in between a parent circle and two L-shaped structures (arrow a).

Table 1. FESEM measured gap width as a function of molecule length and layer count. The single molecule thicknesses calculated from ellipsometry are 1.5 ± 0.1 nm for $HS(CH_2)_{10}COOH$ and 2.0 ± 0.1 nm for $HS(CH_2)_{15}COOH$. Calculated multilayer thicknesses (Calc.) are from ellipsometry; measured gap widths (Expt.) are from FESEM and are averages of 3 to 13 different areas on the samples (*22*).

Molecule	Layers adsorbed	Multilayer thickness (nm)	
		Calc.	Expt.
$HS(CH_2)_{10}COOH$	9	14	17
$HS(CH_2)_{10}COOH$	26	39	42
$HS(CH_2)_{15}COOH$	9	18	18
$HS(CH_2)_{15}COOH$	10	20	21
$HS(CH_2)_{15}COOH$	20	40	32

Because the multilayers are built sideways, the patterns are inherently robust with respect to defects in adjacent layers. One continuous multilayer domain is sufficient to screen defects in adjacent layers on the side of the parent gold trace. Note that the gap location accurately reflects the contours of the parent gold trace (see Fig. 2, D, H, and I). As shown in Table 1 and other measurements, our results for varying initial gap widths, molecular lengths, layer counts, parent structure lengths, and shape show that the gap size is determined by the molecular ruler, whereas the central trace width is determined by the initial gap minus twice the multilayer molecular ruler size. The current limit appears to be the surface quality of the electron beam–generated structures, which are then reproduced or reduced using our method (note the reproduced roughness in our initial demonstrations, as in Fig. 2, D and H). Numerous electrochemical methods exist for making metallic structures smoother and more regular that could conveniently be applied here (*20*). Initial results for the formation of more complex structures within hollow parent structures are shown in Fig. 3.

Our method enables the fabrication of arrays of structures in a single fabrication process, and can be applied to photolithographically prepared parent structures as well. A variety of metals can be used for the constructed patterns (*21*). Moreover, the above results suggest interesting applications of the molecular ruler resist method, such as single molecule adsorption on metal dots, measurements of electron transport in quantum wires and dots, and the construction of closely spaced electrodes for electronic measurements of single molecules.

References and Notes

1. P. Rai-Choudhury, Ed. *SPIE Handbook of Microlithography, Micromachining and Microfabrication* (SPIE, Bellingham, WA, 1997), vol. 1, pp. 139–250.
2. D. Natelson, R. L. Willet, K. W. West, L. N. Pfeiffer, *Appl. Phys. Lett.* **77**, 1991 (2000).
3. S. Y. Chou, P. R. Krauss, W. Zhang, L. Guo, L. Zhuang, *J. Vac. Sci. Technol. B* **15**, 2897 (1997).
4. H. Sugimura, N. Nakagiri, *J. Am. Chem. Soc.* **119**, 9226 (1997).
5. M. A. Reed *et al.*, *Appl. Phys. Lett.* **75**, 624 (1999).
6. S. Hong, J. Zhu, C. A. Mirkin, *Science* **286**, 523 (1999).
7. S. J. Tans, A. R. M. Verschueren, C. Dekker, *Nature* **393**, 49 (1998).
8. E. W. Wong, P. E. Sheehan, C. M. Lieber, *Science* **277**, 1971 (1997).
9. T. W. Ebbesen *et al.*, *Nature* **382**, 54 (1996).
10. B. R. Martin *et al.*, *Adv. Mater.* **11**, 1021 (1999).
11. E. Evans, H. Bowman, A. Leung, D. Needham, D. Tirrell, *Science* **273**, 933 (1996).
12. E. Braun, Y. Eichen, U. Sivan, G. Ben-Yoseph, *Nature* **391**, 775 (1998).
13. Y. Wang, S. Y. Chou, *J. Vac. Sci. Technol. B* **10**, 2962 (1992).
14. S. L. Clark, P. T. Hammond, *Adv. Mater.* **10**, 1515 (1998).
15. S. D. Evans, A. Ulman, K. E. Goppert-Berarducci, J. L. Gerenser, *J. Am. Chem. Soc.* **113**, 5866 (1991).
16. The XPS data are available as Web tables 1 and 2 and Web fig. 1, available at *Science* Online www.sciencemag.org/cgi/content/full/291/5506/1019/DC1.
17. T. van der Boom-Moav, personal communication.
18. J. I. Goldstein, *et al.*, *Scanning Electron Microscopy and X-Ray Microanalysis* (Plenum, New York, 1981) pp. 461–494.
19. As shown in the bottom row of Table 1, the gap in this 20-layer sample is smaller than expected (~32 nm instead of an expected ~40 nm). This difference might be due to changes in packing of the layers after several adsorptions, or to a tilt of the structure.
20. D. J. Trevor, C. E. D. Chidsey, *J. Vac. Sci. Technol. B* **9**, 964 (1991).
21. A. Hatzor, P. S. Weiss, in preparation.
22. In some samples after the lift-off process, the gap was wider than expected from the multilayer borderline. This phenomenon might be the result of annealing of the newly formed metal wire into a more stable, thinner form caused by the lift-off process. These samples were excluded from the calculation.
23. We thank E. Basgall, T. Kuzma, J. Lonjin, and A. Mieckowski for technical assistance and R. Hengstebeck for XPS measurements. We also thank T. Mallouk and R. Davis for helpful discussions and D. Allara for the use of his ellipsometer. Supported by the Army Research Office, the Defense Advanced Research Projects Agency, the National Science Foundation, and the Office of Naval Research.

16 November 2000; accepted 20 December 2000